The temperature-salinity relationship of the mixed layer

R. Ferrari

Woods Hole Oceanographic Institution, Woods Hole, Massachusetts - USA

F. Paparella, D.L. Rudnick and W.R. Young

Scripps Institution of Oceanography, La Jolla, California - USA

Abstract. The surface mixed layer of the ocean is often characterized by density compensation between the horizontal temperature and salinity gradients. In this contribution we present a combination of theoretical arguments and numerical simulations to investigate how compensation might emerge as a result of processes at work within the mixed layer. The dynamics of the mixed layer are investigated through a simple model. The model consists of a pair of coupled advection-diffusion equations for heat and salt. The coupling arises through a nonlinear diffusion operator proportional to the buoyancy gradient, which parameterizes the combined effect of slumping and mixing of small-scale horizontal buoyancy gradients. Numerical solutions of the mixed layer model show that the nonlinear diffusion creates compensation between the temperature and salinity gradients, while the stirring field maintains alignment between the two gradients. The results of this work suggest a new parameterization of the horizontal fluxes of heat and salt for numerical models of the mixed layer.

1. Introduction

Observations show that the thermohaline structure of the surface mixed layer (ML) of the ocean is largely compensated. In other words, temperature and salinity fronts coincide so that the resulting density contrasts are small relative to the individual contributions of heat and salt. This phenomenon has been known for some time for certain fronts at scales of a few tens to one hundred kilometers (*Roden*, 1975; *Rudnick and Luyten*, 1996). Recent high-resolution observations have shown that compensation exists down to horizontal scales of tens of meters in the North Pacific (Rudnick and Ferrari, 1999; *Ferrari and Rudnick*, 2000) and throughout the global ocean on scales of kilometers (*Rudnick and Martin*, 2001). An example from a horizontal tow in the ML of the Subtropical North Pacific is given in Figure 1. Notice how almost all fluctuations of temperature are mirrored in salinity so that density gradients are minimized.

One explanation of these observations is that atmospheric forcing conspires to create and juxtapose water masses with compensating properties. However the ratio of heat to freshwater density fluxes is variable in large scale maps (*Schmitt et al.*, 1989) and in time series at a point (*Weller et al.*, 1985), so internal ocean dynamics is required to account for the observed compensation. *Young* (1994) and *Ferrari and Young* (1997) propose a more satisfactory explanation that relies on regulating mechanisms at work in the ML. These theoretical arguments suggest that compensation is the result of the preferential diffusion of horizontal density gradients which occurs because of the combined action of *unbalanced motions* and *vertical mixing*.

The physical explanation of the theory of Young and collaborators is as follows. Horizontal gradients of temperature and salinity can arise in the ML in response to non homogeneous atmospheric forcing and entrainment of thermocline waters. At some locations temperature and salinity will compensate each other exactly, whereas in other locations temperature and salinity will create strong horizontal density gradients. Much of the ML will lie between these two extremes. The strong density gradients slump under the action of gravity and tend to restratify the ML. Vertical mixing eventually arrests this unbalanced motion by remixing the ML. This mechanism is essentially thermohaline shear dispersion, where the shear is driven by the horizontal density gradient, and the vertical mixing results from the variety of processes that mix the ML. On the other hand, compensated fronts are balanced and therefore do not experience shear dispersion. The net result is that density

fronts are diffused, while compensated fronts persist.

The preferential diffusion of horizontal density gradients can be represented with mixing parameterizations in which the transport of heat and salt depends nonlinearly on the density gradient, e.g., with diffusivities proportional to some power of the density gradient (*Young*, 1994; *Ferrari and Young*, 1997). In this paper we examine the establishment of thermohaline compensation by implementing these nonlinear diffusive parameterizations in a simple model of the ML. Numerical solutions show that the thermohaline structure of the ML is generated by a balance between the mesoscale straining field, that acts to increase temperature and salinity gradients, and the nonlinear diffusion, that arrests the formation of density gradients but not of compensated gradients. In agreement with observations, temperature and salinity gradients tend to be aligned, because both heat and salt are advected by the same straining field, and compensated.

The mechanism of compensation described above implicate vertically sheared currents within the ML and it is not included in numerical models with bulk MLs. In the last section of the paper we show how to simplify the nonlinear diffusive parameterization so that it can be implemented in ocean circulation models to improve the representation of ML thermohaline dynamics.

The paper is organized as follows. In section 2, we revisit the arguments of Young and collaborators in the context of the parameterization of diapycnal fluxes in the ML. In section 3, we describe numerical simulations used to test the nonlinear diffusive parameterization of heat and salt transports in the ML. In section 4, we suggest a simplified version of the nonlinear diffusive parameterization to be implemented in bulk ML models. Finally, conclusions are offered in section 5.

2. Horizontal transport of heat and salt in the mixed layer

Let us consider the dispersion of some tracer of concentration θ in the ML. We model the ML as a vigorously mixed, shallow layer, characterized by a small aspect ratio, i.e., with a depth H much less than the horizontal scale. The main point here is that there are two very different time scales: a fast time scale τ_V over which the layer is mixed vertically over the depth H and a longer time scale τ_H associated with horizontal transports.

The mathematical model for the transport of a tracer θ stirred by an incompressible velocity field $\mathbf{u}$ is the familiar advection-diffusion equation,

$$\partial_t \theta + \mathbf{u} \cdot \nabla \theta = \kappa \nabla^2 \theta, \tag{1}$$

together with appropriate boundary conditions. The operator on the RHS represents the diffusion of tracer fluctuations by molecular motions and κ is the molecular diffusivity. The equation in (1) is appropriate to describe the transport of θ at scales from a few millimeters to thousands of kilometers. However, the resulting description is overly complicated. Our goal is to derive a simpler model that describes transports in the ML at large scales and long times by averaging the equation in (1) over short times and short scales. The key step in the analysis is to find appropriate scales for the averaging so that we can derive a closed equation for the averaged concentration $\bar{\theta}$ by folding all the details of the small scale motions in a suitable operator $\mathcal{D}$ that depends on averaged variables, i.e.,

$$\partial_t \bar{\theta} + \bar{\mathbf{u}} \cdot \nabla \bar{\theta} = \mathcal{D}(\bar{\mathbf{u}}, \bar{\theta}), \tag{2}$$

where $\bar{\mathbf{u}}$ is the averaged velocity field.

Some very popular ML models, referred to as bulk models (e.g. *Kraus and Turner*, 1967), choose to average over the depth H of the ML and the characteristic time of vertical mixing τ_V. This choice is quite natural, because the turbulent fluxes that homogenize vertically the ML are due to processes such as convection and Langmuir cells, characterized by coherent eddies which span the depth H and have an aspect ratio close to one. In these models, the operator $\mathcal{D}$ parameterizes all the processes that maintain the ML well mixed in the vertical. A problem arises when bulk ML are implemented in circulation models that resolve horizontal scales that are orders of magnitude larger than H. In this case one has to average the tracer equation over H in the vertical, but over a scale $L > H$ in the horizontal. A typical solution is to parameterize in series the motions on scales shorter than H and those on scales between H and L[1]. That is, the same operator $\mathcal{D}$ is retained to describe the fluxes that mix vertically the ML, but a lateral effective eddy diffusivity is introduced to parameterize the fluxes at larger scales. Here we show that unbalanced horizontal motions with characteristic scales between H and L act in parallel with the turbulent motions on scales shorter than H. Therefore it is necessary to modify the operator $\mathcal{D}$ and parameterize all unresolved motions together.

Let us average equation (1) over the depth H in the vertical, over a scale $L > H$ in the horizontal and over a time $\tau_H > \tau_V$. The scales L and τ_H have only lower bounds, but are not specified for the moment. We obtain the Reynolds' averaged equation,

$$\partial_t \bar{\theta} + \bar{\mathbf{u}} \cdot \nabla_H \bar{\theta} = -\nabla_H \cdot \overline{\mathbf{u}'\theta'} + \kappa \nabla_H^2 \bar{\theta} + \mathcal{F}. \tag{3}$$

[1]See *Garrett* (2001) for a discussion of parameterizations of unresolved motions in parallel and in series.

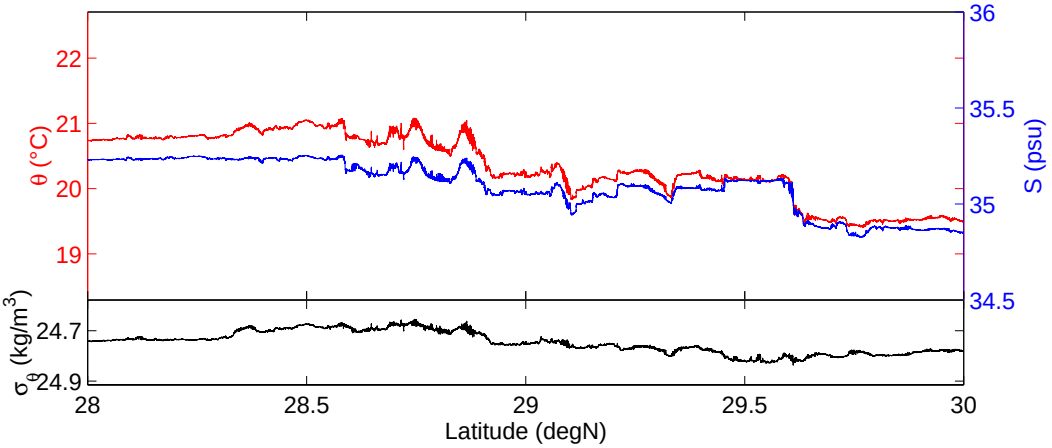

Figure 1. Potential temperature (red line), salinity (blue line) and potential density (black line) from a horizontal SeaSoar tow at 50 m in Subtropical North Pacific, at 140 degrees west, between 28 and 30 degrees north. This depth is in the middle of the local mixed layer. The vertical axis for temperature and salinity are scaled by the respective expansion coefficients so that excursions of temperature and salinity show the change they imply on density.

Here $\bar{\theta}$ and $\bar{\mathbf{u}}$ are the averaged velocity and averaged tracer concentration and θ' and $\mathbf{u}'$ are departures from those averages. $\mathcal{F}$ represents the flux of tracer induced by the boundary conditions at the top and bottom of the ML. The notation ∇_H is used to remind that derivatives are taken only in the horizontal, because the averaged quantities do not depend on the vertical coordinate. In order to simplify the discussion, we assume that H is a constant independent of position (for more on this point see *Young*, 1994; *Garrett and Tandon*, 1997).

The next step is to express the first term on the RHS (called "eddy flux divergence") in terms of averaged quantities. Mixing-length theories are a common way to achieve this goal. The argument goes that a fluid particle carries the value of a conserved, and hence transferable, tracer for some length $\mathbf{l}'$, before it is mixed with its new surroundings. We give a vectorial nature to $\mathbf{l}'$ to allow for situations which are not isotropic. If the particle has a concentration of scalar typical of its surroundings then the eddy flux of tracer θ is given by

$$\overline{\mathbf{u}'\theta'} = -\overline{\mathbf{u}'\mathbf{l}'} \cdot \nabla_H \bar{\theta}, \tag{4}$$

where it is assumed that $\nabla_H \bar{\theta}$ varies little over distances comparable with the mixing length $\mathbf{l}'$. The tensor $\overline{\mathbf{u}'\mathbf{l}'}$ defines the eddy diffusivity.

In the special case when the statistics of the velocity field are homogeneous and isotropic, the eddy diffusivity tensor is a constant, and the eddy transport assumes the form of a down-gradient Fickian diffusion:

$$\overline{\mathbf{u}'\theta'} = -k\nabla_H \bar{\theta}, \tag{5}$$

This kind of closure is commonly applied to ML models and the two relevant scalars (temperature and salinity) are diffused with the same eddy diffusion coefficient, and are independent from each other.

However in the ML there are lateral inhomogeneities in the buoyancy[2] field at scales larger than H. Horizontal buoyancy gradients slump under the action of gravity and drive horizontal eddy fluxes. Therefore we expect the transport of tracer to be in the direction of and to increase with $\nabla_H B$. This breaks the assumptions of homogeneity and isotropy. Therefore a down-gradient Fickian diffusion cannot be used to model the ML at scales larger then H. A more appropriate expression for the diffusivity tensor is,

$$\overline{\mathbf{u}'\mathbf{l}'} = \gamma f(|\nabla_H \bar{B}|) \nabla_H \bar{B} \, \nabla_H \bar{B}, \tag{6}$$

where γ is a constant and $f(|\nabla_H \bar{B}|)$ a non-dimensional function whose form depends on the details of the hydrodynamic instabilities that dominate in the eddy field. The expression (6) is rationalized as follows. According to mixing-length theories, the diffusivity tensor

[2]Buoyancy B is defined as $\rho = \rho_0 \left[1 - g^{-1}B\right]$, where ρ is the fluid's density, ρ_0 is a constant reference density and g is the acceleration of gravity. With this definition, B has the dimensions of acceleration.

can be expressed in terms of the characteristic velocity $\mathbf{v}_{eddy}$ and length $\mathbf{l}_{eddy}$ of the transfer process, that is $\overline{\mathbf{u}'\mathbf{l}'} \propto \mathbf{u}_{eddy}\,\mathbf{l}_{eddy}$. In our case the length scale is given by $\mathbf{l}_{eddy} = \mathbf{u}_{eddy}\,\tau_V$, where τ_V is the time for which the slumping process acts, before it is arrested by the turbulent fluxes that mix vertically the ML. The eddy velocity is in the direction of $\nabla_H \bar{B}$ with a magnitude proportional to $|\nabla_H \bar{B}|$. Thus we get the expression in (6), where the tensor $\nabla_H \bar{B}\,\nabla_H \bar{B}$ arises from the direction of the eddy velocity field and $\gamma f(|\nabla_H \bar{B}|)$ is a positive semidefinite term that determines the magnitude of the flux. Notice that both the unbalanced motions at scales larger than H and the turbulent fluxes at scales shorter than H enter in the closure in 6. That is the processes of slumping and mixing act in parallel.

Plugging (6) into (4) gives the eddy tracer flux,

$$\overline{\mathbf{u}'\theta'} = -\gamma f(|\nabla_H \bar{B}|)\left(\nabla_H \bar{B}\cdot\nabla_H \bar{\theta}\right)\nabla_H \bar{B}. \qquad (7)$$

Notice that, even though the flux is in the direction of $\nabla\bar{B}$, $\overline{\mathbf{u}'\theta'}\cdot\nabla\bar{\theta} < 0$. Thus the flux of tracer tends to be down the tracer gradient, but only the projection of the tracer gradient along the direction of the buoyancy gradient contributes to the flux.

We now apply the closure in (7) to the advection-diffusion equations for heat and salt in the ML,

$$\begin{aligned} \partial_t T \;+\; & \mathbf{u}\cdot\nabla T = \\ =\; & \gamma\nabla\cdot\left[f\big(|\nabla B|\big)\big(\nabla B\cdot\nabla T\big)\nabla B\right] + \mathcal{F}_T, \quad (8)\\ \partial_t S \;+\; & \mathbf{u}\cdot\nabla S = \\ =\; & \gamma\nabla\cdot\left[f\big(|\nabla B|\big)\big(\nabla B\cdot\nabla S\big)\nabla B\right] + \mathcal{F}_S, \quad (9) \end{aligned}$$

where $\mathcal{F}_T$ and $\mathcal{F}_S$ represent the thermohaline fluxes from the top and bottom of the ML. We dropped overbars and we replaced ∇_H with ∇ for convenience, but keep in mind that all variables are averaged over scales larger than H and times longer than τ_V and that derivatives are taken only in the horizontal. We assume a linear equation of state and measure T and S in buoyancy units units, so that,

$$B = T - S. \qquad (10)$$

The nonlinear advection-diffusion equations (8) and (9), together with (10), form a closed system whose solution is fully determined once the forcings $\mathcal{F}_T$ and $\mathcal{F}_S$ and the large scale velocity field $\mathbf{u}$ are prescribed.

By adding and subtracting (8) and (9), we obtain closed equations for buoyancy and spice $V = T + S$ (*Veronis*, 1972; *Munk*, 1981), viz.,

$$\begin{aligned} \partial_t B \;+\; & \mathbf{u}\cdot\nabla B = \\ =\; & \gamma\nabla\cdot\left[f\big(|\nabla B|\big)\big(\nabla B\cdot\nabla B\big)\nabla B\right] + \mathcal{F}_B, \quad (11)\\ \partial_t V \;+\; & \mathbf{u}\cdot\nabla V = \\ =\; & \gamma\nabla\cdot\left[f\big(|\nabla B|\big)\big(\nabla V\cdot\nabla B\big)\nabla B\right] + \mathcal{F}_V, \quad (12) \end{aligned}$$

where $\mathcal{F}_B = \mathcal{F}_T - \mathcal{F}_S$ and $\mathcal{F}_V = \mathcal{F}_T + \mathcal{F}_S$. We can now see how the equations in (11) and (12) model the development of compensation in the ML. The product $f\big(|\nabla B|\big)\big(\nabla B\cdot\nabla B\big)$ must be an increasing function of $|\nabla B|$ to be consistent with our assumption that eddy fluxes are driven by buoyancy gradients. Under this constraint, the nonlinear diffusion always dissipates buoyancy, even more so when $|\nabla B|$ is large. Also spice is dissipated where $|\nabla B|$ is large. However large values of $|\nabla V|$ can survive in regions where $|\nabla B|$ is small. In terms of temperature and salinity this means that compensated fronts, for which $\nabla T \approx \nabla S$ persist, while buoyancy fronts are short lived.

Young (1994) and *Ferrari and Young* (1997) derive formally equations of the form of those in (8) and (9) to parameterize the transport of heat and salt on horizontal scales of a few kilometers in the ML. These theoretical works are examples of the closures we have been discussing when the averaging is done over the depth of the ML, over horizontal scales of a few kilometers and time scales of a few hours. Nonlinear diffusion arises because the horizontal transport of heat and salt is by shear dispersion, and the shear flow doing the dispersion is driven by slumping horizontal buoyancy gradients. The strength of the shear dispersion increases as the horizontal buoyancy gradient squared, that is $f\big(|\nabla B|\big) = 1$ in (8) and (9).

At scales larger than the Rossby radius of deformation *Ro*, unbalanced motions are influenced by rotation in the form of baroclinic instability. Therefore, if one is to parameterize the transport of heat and salt on horizontal scales larger than *Ro*, say 10 km for a typical ML, the closure must include the transports due to eddies generated at baroclinically unstable gradients. *Green* (1970) and *Stone* (1972) derived expressions for the tracer fluxes generated by baroclinic waves. Their results predict that the baroclinic eddy fluxes across a buoyancy gradient are proportional to the absolute value of the diapycnal buoyancy gradient. Green and Stone considered only zonally-averaged models and did not investigate the direction of the fluxes. If their arguments are extended to two horizontal dimensions to parameterize diapycnal fluxes of heat and salt in the ML, one obtains nonlinear diffusion equations of the form in (8) and (9) with $f(|\nabla B|) = |\nabla B|^{-1}$. Notice, however, that a full parameterization of baroclinic instability should include the eddy fluxes along isopycnals as well (*Marshall and Shutts*, 1981). This issue is not pursued further here, because we focus on the role of diapycnal fluxes on the establishment of the temperature-salinity relationship in the ML.

Chris Garrett, during the meeting, suggested that symmetric instability might also drive thermohaline

fluxes in the ML. *Haine and Marshall* (1997) used numerical simulations to study what hydrodynamical instabilities control the transfer of buoyancy through the ML on scales of some tens of kilometers. Their conclusion is that nonhydrostatic baroclinic instability provides the dominant mode of lateral buoyancy transfer. However symmetric instability plays an important role during the slumping process by setting to zero potential vorticity along isopycnal surfaces. Clearly more work need to be done to formulate a closure that takes into account the effects of both symmetric and baroclinic instabilities.

3. Thermohaline alignment and compensation in the mixed layer

The nonlinear advection-diffusion equations in (8) and (9) are now used to investigate how compensation appears in the ML. Suppose that spatial variations in temperature and salinity are created by surface fluxes that vary on large horizontal scales. Mesoscale stirring will create small-scale temperature and salinity gradients by stretching and folding the large scale thermohaline patterns. Large density gradients will disappear quickly as a result of nonlinear diffusion, while compensated gradients will persist for longer times. Thus we expect that the temperature and salinity gradients present at small scales at any particular moment will be typically compensated. We are now going to test this scenario with a numerical model.

3.1. Numerical model

The parameterization in (8) and (9) is tested with numerical simulations in which temperature and salinity are advected using a velocity field generated by solving the equivalent barotropic equations in the streamfunction-vorticity formulation,

$$\partial_t \zeta + J(\psi, \zeta) = -\mu\zeta + \nu\nabla^6\zeta + \mathcal{F}_\zeta, \qquad (13)$$

where ψ is the streamfunction, $\zeta = \nabla^2\psi$ the relative vorticity and J the Jacobian operator. The forcing $\mathcal{F}_\zeta$ is applied in spectral space at a scale of 6 km with constant amplitude and random phases. The bottom drag coefficient is set to $\mu = 3 \cdot 10^{-6}$ s^{-1} and the hyper-viscosity to $\nu = 3 \cdot 10^{6}$ m^6 s^{-1}. The result is a two-dimensional turbulent field with meandering vortices of a diameter of approximately 3 km (half the forcing scale) and RMS velocities of 0.1 m s^{-1} (Figure 2). The domain of integration is a biperiodic square of 51.2×51.2 km^2 with a mesh of 100 m. This is a poor model of the mesoscale dynamics of the ML. In particular we are neglecting feedbacks between the buoyancy and the velocity fields. But our goal is to show that compensation develops at scales small scales, regardless of the details of the stirring field and, in this context, the model in 13 suffices.

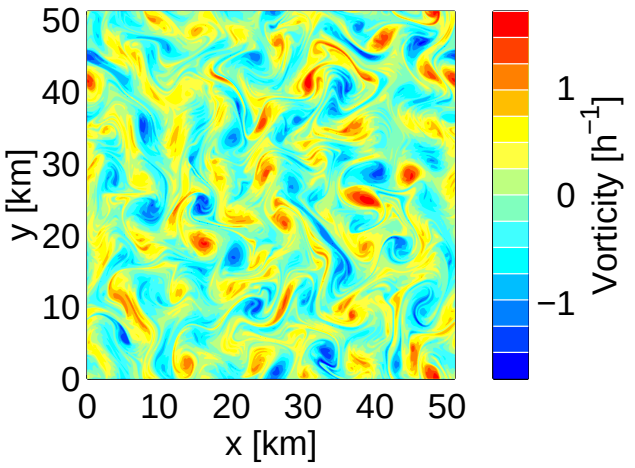

Figure 2. Snapshot of the vorticity field obtained by integrating the equivalent barotropic equations. The typical size of vortices is about 3 km, that is half the wavelength of 6 km at which the vorticity equation is forced.

The temperature and salinity equations in (8) and (9) are integrated with $f(|\nabla B|) = 1$, that is we use the closure in *Young* (1994) and *Ferrari and Young* (1997). The value of γ is set to 10^{14} m^{2}s^3 appropriate for typical ML parameters (details in *Ferrari and Young*, 1997). However the qualitative results discussed in the rest of this paper do not depend on the particular choice of $f(|\nabla B|)$.

Temperature and salinity are forced with orthogonal sinusoidal patterns, that is we set $\mathcal{F}_T = F_0 \cos qx$ in the RHS of (8) and $\mathcal{F}_S = F_0 \sin qy$ in the RHS of (9). The sinusoids have a wavelength equal to the domain size, i.e., $q = 2\pi/51.2$ km^{-1}. The amplitude F_0 is chosen such as to have thermohaline fluctuations of 1°C and 0.35 psu, at the scale of the domain. These forcings do not to impose any correlation between temperature and salinity fluctuations. Further details on the numerical code are given in *Ferrari and Paparella* (2001).

3.2. Complex density ratio

It is common to quantify compensation in terms of the density ratio, defined as the change in buoyancy due to temperature divided by the change in buoyancy due to salinity,

$$R_{1D} \equiv \frac{\hat{\ell} \cdot \nabla T}{\hat{\ell} \cdot \nabla S}, \qquad (14)$$

where temperature and salinity are defined in buoyancy units, and $\hat{\ell}$ is the direction along which the cut is taken.

In two-dimensions, it is convenient to introduce a

complex density ratio as,

$$R \equiv \frac{T_x + \mathrm{i}\, T_y}{S_x + \mathrm{i}\, S_y}. \tag{15}$$

The complex density ratio has both a magnitude and a phase, $R = |R| \exp(\mathrm{i}\phi)$: $|R|$ is the ratio of the magnitudes of the temperature and salinity gradients and ϕ is the angle between them. If the gradients are parallel ($\phi = 0°$) or antiparallel ($\phi = 180°$), there is *thermohaline alignment* and the definition of R in the complex plane is equivalent to that in (14) regardless of the orientation of $\hat{\ell}$. When $|R| > 1$, the change in buoyancy due to temperature is greater than the change in buoyancy due to salinity along the direction of ∇B, that is $|\nabla B \cdot \nabla T| > |\nabla B \cdot \nabla S|$ and the buoyancy-front is temperature-dominated. The opposite is true if $|R| < 1$ and the buoyancy-front is salinity-dominated. The particular case $|R| = 1$ and $\phi = 0°$ describes *thermohaline compensation.*

Because the magnitude of the complex density ratio is infinite when the salinity gradient vanishes, we characterize fronts in terms of the phase ϕ and the Turner angle,

$$\mathrm{Tu} \equiv \arctan |R|, \tag{16}$$

choosing the branch where $0 \leq \mathrm{Tu} \leq \pi/2$. All statistics will be computed in terms of ϕ and Tu. For convenience, results are discussed in terms of ϕ and $|R|$, because their values are more familiar.

In the following we use the joint pdf $\mathcal{P}(\mathrm{Tu}, \phi)$ to describe the degree of alignment and compensation in the ML. The joint pdf is normalized according to

$$\int_0^{\pi/2} \mathrm{d\,Tu} \int_0^{2\pi} \mathrm{d}\phi\ \mathcal{P}(\mathrm{Tu}, \phi) = 1. \tag{17}$$

3.3. Results of numerical simulations

For the simulations we use kilometers to measure distances and hours to measure time. Therefore vorticity is given in h^{-1} and buoyancy in km h^{-2}. We set to zero the initial vorticity, temperature and salinity. After an initial transient of several eddy turnover times, kinetic energy, enstrophy, temperature and salinity variances settle to a constant value; i.e. the system reaches an equilibrium between the variance input by the forcing at large scales and dissipation at small scales.

In Figures 3 and 4, we show snapshots of spice and buoyancy 700 h after the beginning of the simulation. It is difficult to recognize in these snapshots the large scale patterns of buoyancy and spice imposed by the forcing described in section 3.1. But the sinusoidal patterns emerge clearly if one averages the fields over times of the order of a few hundred hours. At small scales the two fields are remarkably different. A comparison of the black contours in the two figures shows that gradients of spice are sharper than those of buoyancy: buoyancy contours are evenly spaced, while spice contours are extremely packed in a few regions and widely spaced in others. Sharp spice gradients with no signature in buoyancy imply $\nabla T \approx \nabla S$, i.e., thermohaline compensation.

The small scale variability in Figures 3 and 4 is produced by stirring the large scale thermohaline patterns. The temperature and salinity gradients, computed across the grid spacing of 100 m, are typically aligned. Alignment occurs because the isolines of T and S are stretched by the same stirring field and thus both tracers end up with gradients pointing in the same directions (*Hua*, 2001). This is shown through the joint pdf $\mathcal{P}(\mathrm{Tu}, \phi)$ (Figure 5). The overwhelming majority of points in the pdf have angles very close to either $\phi = 0°$ or $\phi = 180°$. But this is not the whole story, because not all values of $|R|$ are equally probable along those two angles. The pdf has a clear peak at $R = 1$. This is the signature of nonlinear diffusion which selectively dissipates all gradients whose density ratio is different from one and establishes compensation. Stirring alone does not produce a single peak in the pdf, because it acts only on the relative orientation of ∇T and ∇S but not on the ratio of their magnitudes. This was checked by running a simulation in which the nonlinear diffusion was set to zero. In this limit, the pdf $\mathcal{P}(\mathrm{Tu}, \phi)$ is indeed collapsed along the angles $\phi = 0°$ and $\phi = 180°$, but it does not have a single mode.

Compensation is not maintained always and everywhere in the domain. There are regions, in Figures 3 and 4, where buoyancy and spice gradients are comparable. This happens when the stirring field momentarily creates large buoyancy gradients at small scales. These gradients do not persist for long, though, because nonlinear diffusion restores compensation in a few hours. At any time, a one dimensional cut through the domain shows many compensated fronts and some rare buoyancy fronts. This result agrees with the thermohaline structure found by *Ferrari and Rudnick* (2000) in the ML of the Subtropical North Pacific (Figure 1), where almost all temperature and salinity fluctuations are compensated.

4. Implications for numerical models of the mixed layer

In the previous sections we have suggested that the thermohaline compensation observed in the ML is consistent with preferential diffusion of horizontal buoyancy gradients. The theoretical argument implicates vertically sheared currents within the ML as the agent which produces the preferential horizontal transport of

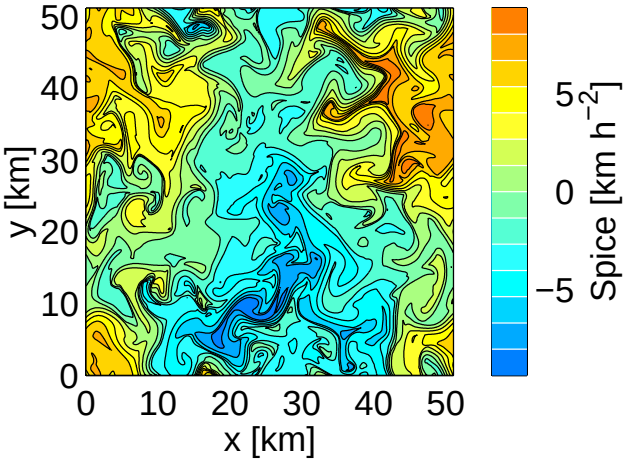

Figure 3. Snapshots of spice at the same time of figures 2 and 4. The colored pattern hints at the large-scale sinusoidal checkerboard, imposed on the spice field through the thermohaline forcing.

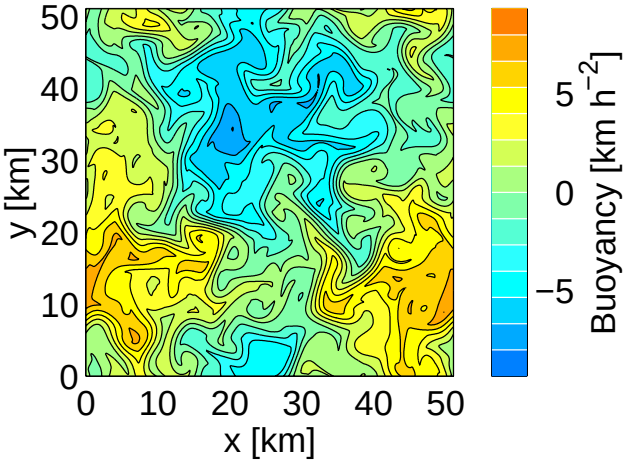

Figure 4. Snapshots of buoyancy at the same time of figures 2 and 3. The colored pattern hints at the large-scale sinusoidal checkerboard, imposed on the buoyancy field through the thermohaline forcing. At small scales buoyancy shows less structure and milder gradients than spice. Regions with large spice fluctuations with no signature in buoyancy are the trademark of compensation.

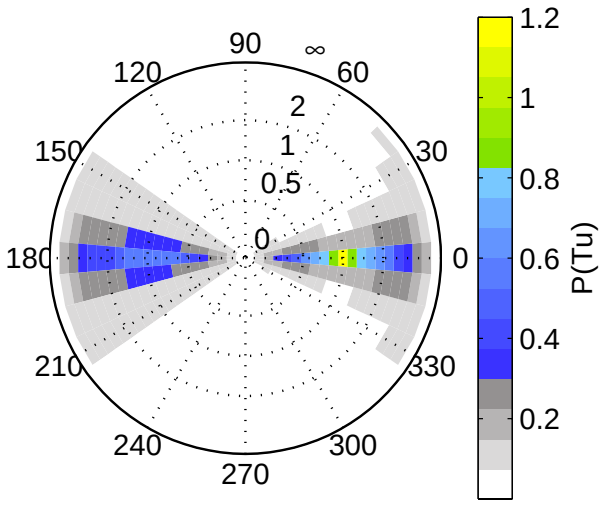

Figure 5. Joint pdf $\mathcal{P}(\mathrm{Tu}, \phi)$ of the complex density ratio R defined in section 3.2. The azimuthal position in the radar plot indicates the angle between the temperature and the salinity gradients, while the radial displacement is the ratio of their magnitudes. The pdf is an average over 200 hours during which the simulation was in equilibrium. Nearly all points lie along the line of alignment, that is at angles $\phi = 0^\circ$ and $\phi = 180^\circ$. The maximum of the pdf is at $R = 1$ and shows that thermohaline fronts are typically compensated.

density. Numerical models with bulk MLs do not include this physics. The purpose of this last section is to suggest a simple parameterization of ML horizontal transports that might improve the representation of thermohaline dynamics in numerical models with bulk ML.

Bulk ML parameterizations ignore the potential energy stored in horizontal buoyancy gradients. But we contend that the release of this potential energy plays an important role in establishing compensation. The system in (11) and (12) describes the horizontal dynamics of the vertically-averaged fields and could be implemented in a bulk ML model. However the nonlinear diffusive terms on the RHS of (11) and (12) are difficult to integrate numerically. In small regions with large buoyancy gradients the diffusive constraint on the time stepping becomes severe (*Ferrari and Paparella*, 2001) and the whole calculation proceeds very slowly. The path we follow here is to derive a substitute model that retains the basic physics of (11) and (12), but that is easy to integrate numerically. That is we write a linear model that diffuses horizontal buoyancy gradients more efficiently than spice gradients in the following way,

$$B_t + \mathbf{u} \cdot \nabla B = \kappa_B \nabla^2 B, \tag{18}$$

$$V_t + \mathbf{u} \cdot \nabla V = \kappa_V \nabla^2 V. \tag{19}$$

By setting $\kappa_B \gg \kappa_V$ buoyancy gradients decay faster than spice gradients. The main advantage of the model in (18) and (19) over that in (11) and (12) is that the diffusivities are independent of the buoyancy gradients and therefore the diffusive constraints on the time stepping do not grow unbounded.

In order to match observations, the two diffusivities κ_B and κ_V must be chosen such that compensation happens mostly at scales below 10 km (*Ferrari and Rudnick*, 2000). That is the dissipation cutoff scale for buoyancy must be of the order of 10 km, while the dissipation cutoff scale for spice must be smaller. The dissipation cutoff scale for buoyancy can be estimated as,

$$L_{diss} \approx \sqrt{\frac{\kappa_B}{\sigma}}, \tag{20}$$

where σ is the RMS strain rate of to the mesoscale eddy field $\mathbf{u}$. A reasonable strain rate in the ML is of the order of 10^{-5} s^{-1}. By imposing $L_{diss} \approx 10$ km, it follows that $\kappa_B \approx 10^3$ m^2 s^{-1}. The choice of κ_V is somewhat arbitrary, but it should be a couple of orders of magnitude smaller than κ_B, so that there is at least a decade between the cutoff scales of spice and buoyancy.

The final step is to write the linear model in (18) and (19) in terms of temperature and salinity, by using once more the linear expressions for buoyancy $B = T - S$ and spice $V = T + S$,

$$T_t + \mathbf{u} \cdot \nabla T = \kappa_+ \nabla^2 T - \kappa_- \nabla^2 S, \tag{21}$$
$$S_t + \mathbf{u} \cdot \nabla S = \kappa_+ \nabla^2 S - \kappa_- \nabla^2 T, \tag{22}$$

where $\kappa_+ = (\kappa_B + \kappa_V)/2$ and $\kappa_- = (\kappa_B - \kappa_V)/2$. The coupling between the salt and heat fluxes in (21) and (22) is formally similar to the Soret and DuFour effects that operate on a molecular level (Caldwell, 1973). The main difference is that, in the present case, all terms in the RHS of (21) and (22) are of the same order and none can be neglected. Only for $\kappa_B = \kappa_V$, the coupling between temperature and salinity disappears.

The parameterization in (21) and (22) has been tested by integrating the equations with the velocity field and thermohaline forcings described in section 3.1. The lower panel of Figure 6 shows the pdf of the meridional density ratio at a scale of 3 km obtained with the linear model. The pdf has a clear peak at $R = 1$, as in the observations (upper panel of Figure 6). Notice that the large scale density ratio for the same simulation is uniform. Thus compensation is a result of the parameterization in (21) and (22), and is not due to the external forcing.

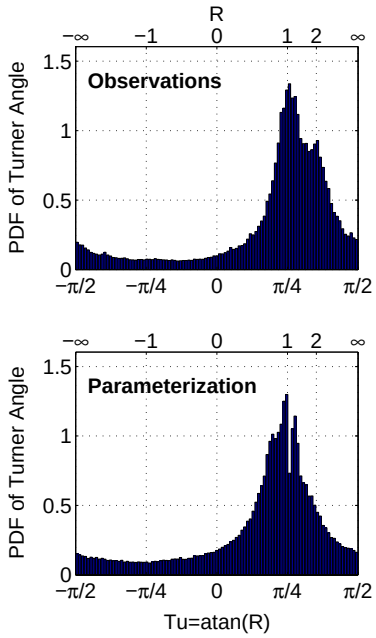

Figure 6. Probability density function of the horizontal mixed-layer Turner angle across a distance of 3 km along 25-35 degrees in the North Pacific (upper panel) and across the same distance in a simulation with the proposed mixed layer parameterization (lower panel). The values of Turner angle and density ratio are indicated on the upper and lower axes. The pdfs have a peak close to $R = 1$ and represent thermohaline fields characterized by buoyancy compensation.

5. Conclusions

We have shown that the ubiquitous compensation of thermohaline gradients observed in the ML is consistent with the theoretical arguments of *Young* (1994) and *Ferrari and Young* (1997). Compensation can be explained as the preferential diffusion of horizontal buoyancy gradients which occurs because unbalanced motion due to these gradients is stronger in the ML than in the more nearly geostrophic interior. The horizontal pressure gradients associated with the buoyancy gradients produce "exchange flows" which act to restratify the ML in the vertical. The turbulent fluxes, that continuously mix the ML in the vertical, oppose the restratification and weaken the horizontal buoyancy gradients. This process is essentially shear dispersion of buoyancy, where the shear flow is driven by the density gradients themselves.

The theoretical arguments of Young and collaborators implicate that eddy fluxes of heat and salt in the ML are in the direction of the buoyancy gradients and act to weaken the horizontal buoyancy stratification. That is, the thermohaline diapycnal fluxes remove the energy stored in horizontal buoyancy gradients. The sit-

uation is reversed below the ML base, where the available potential energy is believed to be removed by adiabatic processes. The difference in the two cases is that there are strong diabatic motions in the ML at small scales, while flows are mostly along isopycnals in the ocean interior. Expressions like the one in (7) might be a first step toward a better parameterizations of diapycnal fluxes in the ML.

We implemented the nonlinear diffusive parameterization of heat and salt in a simple, idealized model of the ML. Numerical simulations showed that buoyancy-driven diffusion is complemented and locally enhanced by the mesoscale stirring field. The strain in the velocity field continuously creates thermohaline gradients at small scales. Nonlinear diffusion selectively removes buoyancy gradients. As a result at any single time typical temperature and salinity gradients are compensated, in agreement with the observations of *Ferrari and Rudnick* (2000). Our model does not include any feedback between the velocity field and buoyancy, as due to rotation. An obvious direction for future research is to investigate whether this feedback plays an important role in the establishment of the temperature-salinity relationship of the ML.

Our discussion emphasized the role of diapycnal fluxes in removing horizontal buoyancy gradients. A question arises as to what maintains the long-lived buoyancy fronts observed at some locations in the ML (e.g. *Roden*, 1975; *Rudnick and Luyten*, 1996). First, these fronts have horizontal scales of a few tens of kilometers. The buoyancy-driven fluxes, discussed above, are mostly active at scales shorter than, say, 10 kilometers and are weaker at larger scales. Second, ML fronts are believed to be maintained by surface forcing or by convergences in the velocity field. When this is the case, the diapycnal thermohaline fluxes do not remove completely the buoyancy gradient. Instead an equilibrium is reached between nonlinear diffusion and forcing. The result is a buoyancy front in which temperature and salinity partly oppose each other, but do not compensate. Observations indeed show partial cancellation of the thermohaline components at many ML fronts.

We also derived a linear model that reproduces the preferential diffusion of horizontal buoyancy gradients. The linear parameterization produced realistic distributions of the density ratio in a simple, idealized model of the ML. It remains an open question whether the new parameterization would produce realistic diapycnal fluxes and water mass conversions, if implemented in high-resolution ocean models with bulk ML.

Acknowledgments. Ferrari wishes to acknowledge the support of the National Science Foundation (OCE96 – 16017) and the WHOI Postdoctoral Fellowship. Ferrari, Rudnick and Young wish to express their thanks to Chris Garrett and Peter Müller for organizing and inviting us to the 'Aha Huliko'a Hawaiian Winter Workshop.

References

Caldwell, D.R., Thermal and Fickian diffusion of sodium chloride in a solution of oceanic concentration, *Deep-Sea Res.*, *20*, 1029–1039, 1973.

Ferrari, R., and W. R. Young, On the development of thermohaline correlations as a result of nonlinear diffusive parameterizations, *J. Mar. Res.*, *55*, 1069–1101, 1997.

Ferrari, R., and Rudnick, D.L., Thermohaline structure of the upper ocean. *J. Geophys. Res.*, *105*, 16857–16883, 2000.

Ferrari, R., and Paparella, F., Compensation and alignment of thermohaline gradients in the mixed layer, in preparation for *J. Phys. Oceanogr.*, 2001.

Ferrari, R., D.L. Rudnick, and W.R. Young, Parameterization of horizontal diffusivities in the mixed layer, in preparation for *J. Phys. Oceanogr.*, 2001.

Garrett C., and A. Tandon, The effects on water mass formation of surface mixed layer time-dependence and entrainment fluxes, *Deep-Sea Res.*, *44*, 1991–2006, 1997.

Garrett, C., Stirring and mixing: what are the rate controlling processes?, in *From stirring to mixing in a stratified ocean*, Proceedings of the 12th 'Aha Huliko'a Hawaiian Winter Workshop, in press, 2001.

Green, J.A., Transfer properties of the large-scale eddies and the general circulation of the atmosphere, *Quart. J. Roy. Meteorol. Soc*, *96*, 157–185, 1970.

Haine T.W.N., and J. Marshall, Gravitational, Symmetric, and Baroclinic Instability of the Ocean Mixed Layer, *J. Phys. Oceanogr.*, *28*, 634–658, 1997.

Hua, B.L., Tracer cascade in geostrophic turbulence, in *From stirring to mixing in a stratified ocean*, Proceedings of the 12th 'Aha Huliko'a Hawaiian Winter Workshop, in press, 2001.

Kraus, E.B., and J.S. Turner, A one dimensional model of the seasonal thermocline, II. The general theory and its consequences, *Tellus*, *19*, 98–105, 1967.

Large, W.G., G. Danabasoglu, S.C. Doney, and J.C. McWilliams, Sensitivity to surface forcing and boundary layer mixing in a global ocean model: Annual-mean climatology, *J. Phys. Oceanogr.*, *27*, 2418–2447, 1997.

Marshall J., and J. Schutts, A note on rotational and divergent eddy fluxes, *J. Phys. Oceanogr.*, *11*, 1677–1680, 1981.

Mellor G.L., and T. Yamada, A hierarchy of turbulent closure models for planetary boundary layers, *J. Atmos. Sci.*, *31*, 1791–1806, 1974.

Munk, W., *Evolution of Physical Oceanography,* (B.A. Warren and C. Wunsch, eds.), Chapter 9. MIT Press, Cambridge, Massachusetts. 198.

Roden, G.I., On north Pacific temperature, salinity, sound velocity and density fronts and their relation to the wind and energy flux fields, *J. Phys. Oceanogr.5*, 557–571, 1975.

Rudnick, D. L., and J. R. Luyten, Intensive survey of the Azores Front, 1, Tracers and dynamics, *J. Geophys. Res.101*, 923-939, 1996.

Rudnick, D.L., and J.P. Martin, On the horizontal density ratio in the upper ocean, submitted to *Dynamics of the Oceans and the Atmosphere*, 2001.

Rudnick, D.L., and R. Ferrari, Compensation of horizontal temperature and salinity gradients in the ocean mixed layer, *Science*, *283*, 526–529, 1999.

Schmitt, R. W., P. S. Bodgen, and C. E. Dorman, Evaporation minus precipitation and density fluxes for the North Atlantic, *J. Phys. Oceanogr.9*, 1208–1221, 1989.

Stommel, H., A conjectural mechanism for determining the thermohaline structure of the oceanic mixed layer, *J. Phys. Oceanogr.*, *23,* 142–148, 1993.

Stone P.H., A simplified radiative-dynamical model for the static stability of rotating atmosphere, *J. Atmos. Sci.*, *96*, 157–185, 1972.

Veronis, G., On properties of seawater defined by temperature, salinity and pressure. *J. Mar. Res., 30,* 227–255, 1972.

Weller, R.A., J.P. Dean, J. Marra, J.F. Price, E.A. Francis, and D.C. Boardman, 3-dimensional flow in the upper ocean, *Science*, *227*, 1552–1556, 1985.

Young, W.R., The subinertial mixed layer approximation, *J. Phys. Oceanogr.*, *24*, 1812–1826, 1994.

R. Ferrari, Woods Hole Oceanographic Institution, MS#21, Woods Hole, Massachusetts, USA. (e-mail: rferrari@whoi.edu)

This preprint was prepared with AGU's LaTeX macros v4, with the extension package 'AGU^{++}' by P. W. Daly, version 1.6a from 1999/05/21, with modifications by D. E. Kelley, version 1.0 from 2001/03/26, for the *'Aha Huliko'a* Hawaiian Winter Workshop.